Available online at www.sciencedirect.com

ScienceDirect

Underground Space xxx (xxxx) xxx

www.elsevier.com/locate/undsp

Practical configured microtremor array measurements (MAMs) for the geological investigation of underground space

Taeseo Ku [a,*], Subramaniam Palanidoss [a], Yunhuo Zhang [a,b], Sung-Woo Moon [a,c], Xiao Wei [a], Ean Seong Huang [d], Jeyatharan Kumarasamy [b], Kok Hun Goh [e]

[a] Department of Civil and Environmental Engineering, National University of Singapore, Singapore
[b] Geotechnical and Tunnel Division, Land Transport Authority, Singapore
[c] Department of Civil and Environmental Engineering, Nazarbayev University, Kazakhstan
[d] Geosystems, Land Transport Authority, Singapore
[e] Infrastructure Design and Land, Land Transport Authority, Singapore

Received 16 November 2019; received in revised form 28 January 2020; accepted 28 January 2020

Abstract Underground space utilization is becoming increasingly essential for modern metropolitan cities such as Singapore. Mapping a soil/rock interface using traditional borehole investigation methods is expensive and difficult, owing to the numerous physical constraints within a built-up city. Boreholes are often far apart, resulting in many unforeseen ground conditions during subsequent excavation. Geophysical methods are sometimes employed as possible alternatives for fast, economical, and efficient bedrock surveys. The goal of this study is to investigate the practical details of applying microtremor array measurement (MAM) as a non-invasive surface wave survey for mapping soil/rock interfaces in Singapore. Critical configurations in field data acquisition are examined, and practical recommendations for array construction are provided. In addition, 30 in situ MAM tests are carried out for two major geological formations in Singapore. From the results, a standard shear wave velocity (V_s) of 500 m/s is found to be suitable for interpreting the soil/rock interface, for the Bukit Timah Granite and Jurong formations. However, the method does not predict well when soft Kallang formation deposits are present. Other limitations are also discussed in the later parts of this paper. Conclusions and practical recommendations are discussed, providing constructive guidance to the industry. The proposed V_s-based method and associated guidelines and limitations can be used to create a digital geological database and are especially useful for rock profiling in an urban environment.

Keywords: Array configuration; MAM; Non-invasive site investigation; Soil/rock interface; Surface wave survey

1 Introduction

Underground space utilization is becoming increasingly essential for modern metropolitan cities such as Singapore. Moreover, many new underground infrastructures are being planned in Singapore. In view of this, profiling and/or mapping of soil/rock interfaces is essential for various geotechnical and environmental applications. In a local context, the rock is defined as a "Grade III" rock. The soil/rock interface denotes the top of the Grade III rock. Investigation of the soil/rock interface is important; it is an essential input in design and analysis (Xiang et al., 2018; Zhang et al., 2019). Current practices for site investigation are based on conventional borehole drilling, which involves traditional drilling, in situ testing, sampling, and laboratory testing. Mapping of a soil/rock interface using traditional borehole investigation is expensive, time consuming, and often difficult, owing to the numerous physical constraints within a built-up city. Boreholes are often spaced far apart, resulting in a higher risk of encountering unforeseen ground conditions during future excavations.

* Corresponding author.
E-mail addresses: ceekt@nus.edu.sg (T. Ku), zhang_yunhuo@lta.gov.sg, zhangyunhuo@u.nus.edu (Y. Zhang), sung.moon@nu.edu.kz (S.-W. Moon), ceewx@nus.edu.sg (X. Wei), huang_eng_seong@lta.gov.sg (E.S. Huang), jeyatharan_kumarasamy@lta.gov.sg (J. Kumarasamy), goh_kok_hun@lta.gov.sg (K.H. Goh).

https://doi.org/10.1016/j.undsp.2020.01.004

Geophysical methods are sometimes employed as possible alternatives for fast, economical, and efficient soil/rock interface surveys. The geotechnical applications of different geophysical methods and their limitations are well-documented in other studies (e.g., Anderson, Croxton, Hoover, & Sirles, 2008). It is noted that seismic geophysical testing methods such as refraction, reflection, multichannel analysis of surface waves (MASW), microtremor array measurement (MAM), ground penetrating radar, electromagnetic surveys, and electrical resistivity approaches can be used for bedrock mapping. However, each of those methods has limitations, such as regarding the applicable depth range, resolution of results, constraints on the presence/absence of seismic noise, and effects of the underground electric cables, urban environment, and ground water table. In an urban environment, MAM methods (also known as passive MASW) are mostly preferred, owing to their applicable depth range and ability to avoid interference from underground cable lines. Moreover, as a non-destructive geophysics approach, MAM can be conducted in an environmentally friendly manner in the urban area. Considering all the noted issues, this study is intended to explore a non-invasive MAM approach for identifying soil/rock interfaces using passive surface wave experiments.

The MAM tests were conducted at the same site using "L"-, circular-, and angular-shaped arrays, to study the effects of array shape. Upon evaluating a suitable array shape, a comprehensive in situ testing scheme was conducted, involving 30 sites in two major local geological formations (Bukit Timah Granite formation and Jurong sedimentary formation). Based on the MAM tests and corresponding bore-log data, a suitable methodology was established for identifying the depth of a rock interface. In addition, the effects of heavy vehicle movement and soft soil layers on the MAM test were also discussed, and separate guidelines were drawn for detecting the depth of the rock interface. The proposed methodology and associated guidelines will be helpful for creating a digital geology database, e.g., for mapping a rock interface with limited existing drilling boreholes.

2 Theory of microtremor array measurement (MAM)

In recent decades, various construction methods for dispersion images and different inversion methods have been well established (Nazarian & Stokoe, 1984; Park, Miller, & Xia, 1999; Tokimatsu, Shinzawa, & Kuwayama, 1992; Zhang, Li, & Ku, 2019; Zhang, Li, Zhang, & Ku, 2019). A dispersion image in the frequency–phase velocity domain is the most popularly used in geotechnical engineering. For instance, one study tested the efficacy of a spatial autocorrelation method for detecting the depth of deeper bedrock (Okada & Suto, 2003). The application of MAM tests in shallow- to medium-depth rock sites by using a shear wave velocity profile has also been evaluated (Hayashi, 2008; Moon, Hayashi, & Ku, 2017a; Moon and Ku, 2017b; Moon, Subramaniam, Zhang, Vinoth, & Ku, 2019). In the present study, a dispersion image (phase velocity versus frequency) was constructed using an extended spatial autocorrelation (ESAC) method (Ling, 1993) derived from the original spatial autocorrelation method (Aki, 1957). Instead of keeping the array radius as the constant term, the ESAC method keeps the frequency as the constant in the calculation of the apparent phase velocity. This can possibly eliminate a restriction in the use of the L-shaped array.

The following steps are involved in the construction of a dispersion image using the ESAC method (Galiana-Merino et al., 2016).

For "N" number of geophones, the normalized cross-spectra ($\rho_{jn}(f)$) is calculated for a pair of geophones using the following expression:

$$\rho_{jn}(f) = \frac{\frac{1}{W}\sum_{w=1}^{W} Re\left\{S_{jn}^{w}(f)\right\}}{\sqrt{\frac{1}{W^2}\sum_{w=1}^{W} S_{jj}^{w}(f)\sum_{w=1}^{W} S_{nn}^{w}(f)}}. \quad (1)$$

Here, f is the frequency (in Hz); S_{jn}^{w} is the cross-spectrum between the j^{th} and n^{th} geophones for each w^{th} segment; S_{jj}^{w} and S_{nn}^{w} are the power spectra at stations j and n, respectively; and W is the number of segments.

The normalized cross-spectra between a possible combination of geophones can be computed as

$$\rho(f,r) = \left\{\rho_{jn}(f)\right\}. \quad (2)$$

In the above, r represents the distance between the geophones, and j and n indicate the possible combination of geophones. Aki (1957) demonstrated that an azimuthally averaged space-correlation has the shape of a Bessel function, J_0, as follows:

$$\rho(f,r) = J_0\left(\frac{2\pi fr}{c(f)}\right). \quad (3)$$

Here, $c(f)$ is the Rayleigh wave phase velocity, which can be estimated iteratively. Thus, for every frequency, the phase velocity can be calculated. The maxima correspond to the measured dispersion curve.

3 Singapore geology

The geological and geotechnical characteristics of the two main geologic formations in this study are listed in Table 1. Both the Bukit Timah Granite and Jurong formations exhibit various weathering conditions and site-specific bedrock locations (e.g., geological spatial variability). Thus, an accurate geotechnical interpretation of the residual soils and rocks from various weathering degrees is crucial for ongoing and potential underground construction activities.

The Bukit Timah Granite formation occupies one third of Singapore and belongs to the early to middle Triassic age (250–235 myr). It consists of granite as a major share, and of granodiorite, adamellite, and diorite in minor quan-

Please cite this article as: T. Ku, S. Palanidoss, Y. Zhang et al., Practical configured microtremor array measurements (MAMs) for the geological investigation of underground space, Underground Space, https://doi.org/10.1016/j.undsp.2020.01.004

Table 1
Geological and geotechnical characteristics (Zhao et al., 1999).

Bukit Timah Granite formation	Jurong formation
• Weathering is extensive, mainly decomposition. • Depth varies between a few m to 80 m. • Undulating bedrock surface with sharp change from residual soil to granite. • The granite rock mass is mostly of good (and above) quality but varies by location.	• Most of the rocks of the Jurong formation are weak. • Rock mass quality is generally below good, i.e., mostly fair to poor, owing to intensive fracturing and low strength. • Rock type and quality can vary rapidly, owing to folded rock layers. • Relatively high permeability owing to fractures.

tities. The weathering of Bukit Timah Granite formation is very extensive owing to tropical rainfalls, with depths varying from a few to 80 m (mostly 20–50 m). Field observations indicate that the grain size increases with depth. As a result of this, the weathering becomes less intensive, and the soil layer clay content is reduced with depth. Based on the weathering classifications of different grades of granite rock (as listed in BSI, 1999), the Bukit Timah Granite formation is classified from Grade VI (residual soil) to Grade I (Intact rock). This formation also features an undulating rock surface with a sharp change from residual soil (Grade VI) or completely weathered material (Grade V) to slightly weathered (Grade II) or fresh granite (Grade I), whereas the highly weathered (Grade IV) and moderately weathered layers (Grade III) are often missing.

The Jurong formation is spread over the west and southwest parts of Singapore and includes a variety of sharply folded sedimentary rocks, such as mudstone, sandstone, shale, conglomerate, phyllite, slate, and limestone. The Jurong formation was formed between the late Triassic (235 myr) and late Jurassic (175 myr) (Zhao, Liu, Lee, Choa, & Teh, 1999). The formation has been severely folded and faulted in the past because of tectonic movement, causing spatially rapid variations in the rock types. The Jurong formation is subject to intensive weathering, owing to the humid tropical climatic conditions in Singapore. The mineral composition of the rocks serves as a key factor influencing the weathering. The depth of the weathered soils ranges from a few meters to approximately 50 m, but the rocks at greater depths may also suffer from the effects of weathering. According to the British Classification system (BSI, 1999) discussed above, the Jurong formation is classified from Grade VI to Grade I, where Grade VI denotes highly weathered residual soil, and Grade I is intact rock. The engineering properties of the rock vary remarkably with different rock types and grades of weathering. Five different types of geomaterials are found in the Jurong formation: residual soil, limestone, sandstone, siltstone, and mudstone (Subramaniam, Zhang, & Ku, 2019).

4 Methodology

This section describes the methodology of this study, covering the effects of array configurations on the field data acquisition, signal processing, and results interpretation for soil/rock interfaces.

4.1 Field data acquisition

Two-dimensional (2D) arrays provide the most rigorous distribution of data points for analysis. For an L-shaped array (Fig. 1(a)), a 90-degree angle is maintained between two legs, and both legs of the array usually have the same length. The L-shaped array is easier to set up in the field than the other shapes of the 2D array. For the angular arrays, the angles between both legs of the array vary between 45° and 135°. The resultant V_s profile in each of the 2D configurations will be an average over the array. Thus, the V_s profile will correspond to the center of a constructed configuration (e.g., the center of a triangle or circle, or the origin of two linear branches in an L-shape).

The average dispersion curves and V_s profiles calculated from MAM tests at the same site using the L-shaped array (90°) and a conventional circular array are compared in Fig. 2. In Fig. 2, two similar phase velocities are determined from using the L-shaped array and circular array. From Fig. 2, it can be concluded that the MAM tests with the L-shaped array (90°) and circular array are equally useful for obtaining a reliable V_s profile that can be utilized to determine the approximate soil/rock interface (within an approximately 5 m resolution in this study).

For more practical applications, the L-shaped array is used. In this study, the effect of the L-shape angle is investigated, in the context of accommodating more flexible site-specific applications (e.g., 135°, 90°, 45°). It may not be always possible to set up an L-shaped array in the field with a 90° spread. Hence, it is necessary to study the effects of the angular arrays. In this study, angular arrays with intended angles of 45° and 135° were constructed, and each obtained V_s profile was compared with the results of the reference L-shaped configuration. Figure 3 shows a sketch of different L-shaped array angles, as determined from a real field testing.

The average dispersion curves and V_s profiles calculated from the MAM tests using the L-shaped array (90°) and angular arrays (45° & 135°) are compared in Fig. 4. The two phase velocities obtained from the L-shaped array and 135° angular array demonstrate a similar trend, with a small change in the frequency shift. In contrast, the testing result from the angular array of 45° shows a much flatter dispersion curve with a higher frequency range. Similarly, the two V_s profiles calculated from the L-shaped array (90°) and angular array of 135° match well.

Please cite this article as: T. Ku, S. Palanidoss, Y. Zhang et al., Practical configured microtremor array measurements (MAMs) for the geological investigation of underground space, Underground Space, https://doi.org/10.1016/j.undsp.2020.01.004

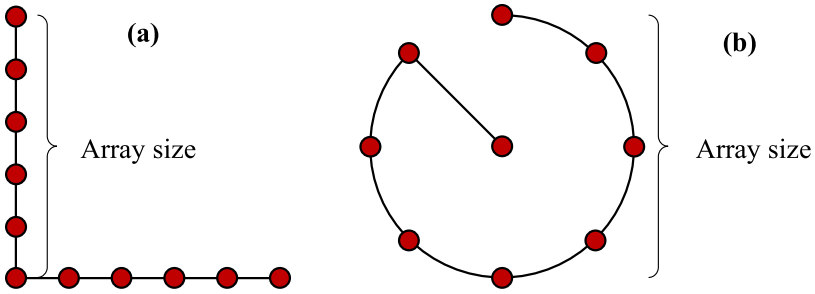

Fig. 1. Map view of microtremor array measurement (MAM) survey.

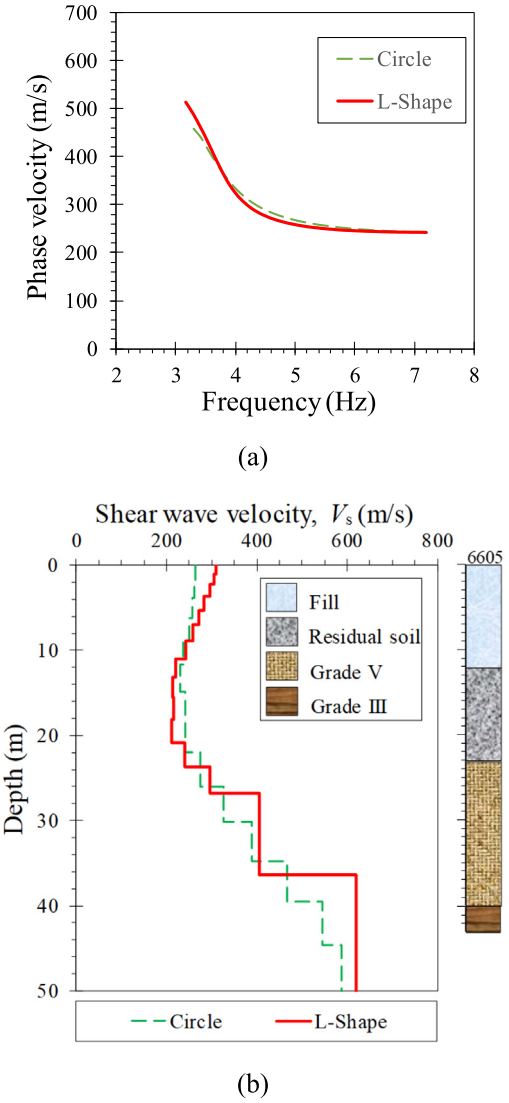

Fig. 2. (a) Comparison of average phase velocities with different array shapes, (b) Comparison of average shear wave velocity profiles with different array shapes.

However, the V_s profile obtained from the MAM test with an angular array of 45° is larger above a depth of 25 m and lower below a depth of 25 m as compared to the other two V_s profiles (90° and 135°). This may be because the angular array of 45° is insufficient for recording the propagated signals in the geophones from the various sources of microtremors and energy radiation from many directions. It is observed that the two similar V_s profiles (90° and 135°) changed suddenly near the boundary layer between the residual soil and completely weathered rock (Grade V), and between the completely weathered rock and moderately weathered rock (Grade III) below the depth of 20 m. Thus, angles of 90° to 135° (between the branches of the L) are recommended for reliable V_s profiling, and for the estimation of suitable bedrock locations. Based on our parametric study in the above investigation, we summarize the recommendations for field data acquisition in Table 2.

4.2 Interpretation of soil/rock interface

Based on the MAM testing results (summarized in the later parts of this paper), a V_s of 500 m/s is used as a reference velocity for estimating the soil/rock interface. After acquisition of the surface wave data from the ambient noise, we need to determine and extract a dispersion curve using signal processing, as introduced in the previous section. This section focuses on interpretation of the soil/rock interface, based on the V_s profile inverted from the dispersion curve. There are several classic inversion algorithms for generating the V_s profile. In this study, the inversion is performed using a genetic algorithm (Dal Moro, Pipan, & Gabrielli, 2007). The method chooses the best model through a misfit function among the chosen models. The chosen models are randomly generated from a specified number of populations and generations. The initial V_s model is usually derived using Eq. (4) to facilitate the inversion process (Brown, Diehl, & Nigbor, 2000):

$$V_s = 1.1V_R \text{ at } z = \frac{\lambda}{3}. \quad (4)$$

Here, V_R is the Rayleigh wave phase velocity, and z and λ denote the depth of the layer and corresponding wavelength, respectively. The V_s profile of the best model (corresponding to the lowest misfit), generated in the inversion process, is further analyzed to find the rock interface. To locate the depth of the rock in a particular grade, a series of MAM tests are conducted in known bore-log locations. By comparing the bore-log information with the V_s

Please cite this article as: T. Ku, S. Palanidoss, Y. Zhang et al., Practical configured microtremor array measurements (MAMs) for the geological investigation of underground space, Underground Space, https://doi.org/10.1016/j.undsp.2020.01.004

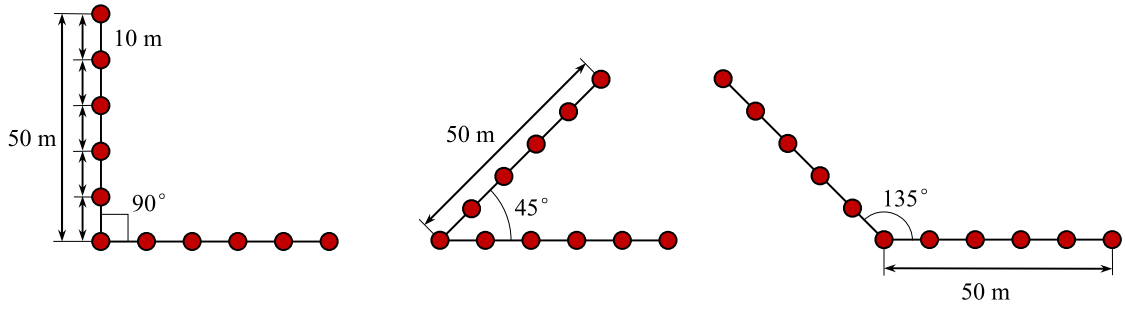

Fig. 3. Sketch of L-shaped array in different angles (90°, 45°, and 135° with 50 m × 50 m array length).

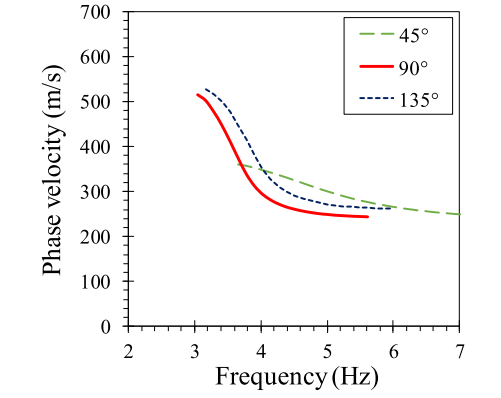

(a)

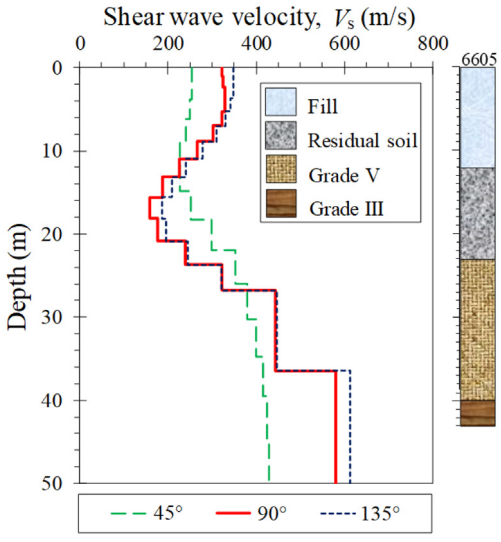

(b)

Fig. 4. (a) Comparison of average phase velocities with different angles, and (b) Comparison of average shear wave velocity profiles with different angles.

profiles, a reference V_s of a particular rock grade can be found. This V_s is used as a guide value for locating the depth of rock where bore-log data is unavailable.

We demonstrate the proposed method with an example. A typical procedure for locating a particular grade of rock is graphically presented in Fig. 5. The present study aims to locate the Grade III rock in the Bukit Timah Granite formation or Jurong formation. The borelog profile and V_s profile are plotted together, as shown in Fig. 5. With the aid of the borelog data, a horizontal line is drawn from the top surface of the Grade III rock to the V_s profile. The actual bedrock depth is compared to the estimated depth using a certain preselected V_s value (e.g., blue line −450 m/s). Similarly, the procedure is repeated for additional sites, to consider the variability in the V_s values of the rock. From this analysis, a reasonable and unique V_s value is determined. For the present case and considering all the initial test sites, 500 m/s is found to be the applicable V_s value of the rock interface between Grade III and Grade IV. Thereafter, this 500 m/s is considered as the guide value for locating Grade III rock where (and/or when) borelog information is unavailable. As shown in Fig. 5, a vertical line is drawn from 500 m/s, and the intersection point in the V_s profile gives the depth of the bedrock (12.2 m).

5 Results

This investigation focuses on identifying the soil/rock interface in the Bukit Timah Granite and Jurong sedimentary formations. A series of MAM tests were extensively conducted across these two geological formations of Singapore (Fig. 6).

5.1 Bukit Timah Granite Formation

In the investigation, 15 MAM tests were conducted in the region of the Bukit Timah Granite formation. As mentioned earlier, a shear wave velocity (V_s) of 500 m/s was used to detect the soil/rock interface. Table 3 summarizes the actual soil/rock interface, and the deviation from the estimation using the preselected V_s-based approach. Figure 7 compares the actual soil/rock interface (depth of Grade III rock from borehole information) with the estimated soil/rock interface from the preselected V_s-based approach.

A statistical analysis is conducted to quantify the accuracy and evaluate the performance of the MAM approach.

Please cite this article as: T. Ku, S. Palanidoss, Y. Zhang et al., Practical configured microtremor array measurements (MAMs) for the geological investigation of underground space, Underground Space, https://doi.org/10.1016/j.undsp.2020.01.004

Table 2
Recommendations for field data acquisition.

Parameter	Setting	Recommendation
Array configuration	(1) Reference tests: L-shaped (e.g., 30 m × 30 m), Circle (D = 30 m)	(1) L-shaped is recommended for the simplicity of testing.
	(2) Array length is approximately the same as depth of interest (i.e., bedrock depth = 30 m)	(2) Array length should be the same as the depth of interest or larger.
	(3) Effect of L-shaped angle: 135°, 90°, 45°	(3) L-shape angles of 90°–135° are recommended.

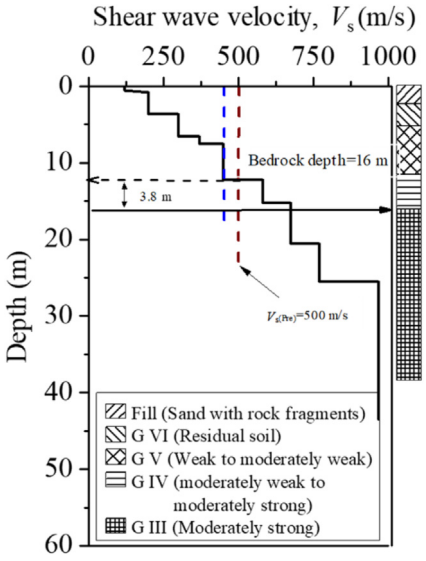

Fig. 5. Typical illustration of the preselected V_s-based method.

Based on the one-to-one plot as shown in Fig. 7, hypothesis testing is conducted for examining if the prediction is equivalent to the actual measurement, with a significance level (normally 0.05). Normality tests are conducted to determine if the prediction difference is normally distributed. Both P-value and graphical methods are used for the hypothesis test for the normality check. Regarding the P-values, all cases are approximately 0.9, which indicates passage of the test. The graphical method also indicates passage of the normality check (Fig. 8). To establish a sense of accuracy as associated with the confidence probability, the confidence interval is calculated. Prior to the confidence interval derivation, the prediction effort must be confirmed to be normally distributed. From the normality test, it is confirmed that the prediction approximately follows a normal distribution, with a mean of −2 m and a standard deviation of 3.8 m. Figure 8(a) shows the cumulative probability density plot, with a 95% confidence interval. Figure 8(b) is the histogram plot of the frequency of the prediction error and the fitted normal distribution probability plot.

As the prediction error is confirmed as following a normal distribution, a one-sample t test is conducted to determine the confidence of the mean, assuming that the variance is unknown. One-sample testing for the variance

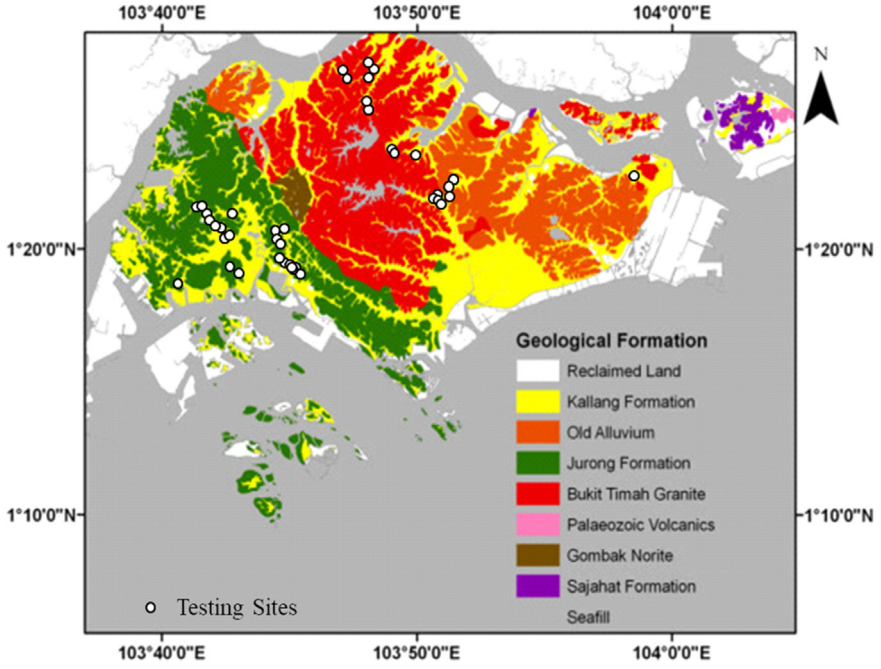

Fig. 6. Testing locations in the Bukit Timah Granite formation and Jurong formation region (modified from Woon & Yingxin, 2009).

Please cite this article as: T. Ku, S. Palanidoss, Y. Zhang et al., Practical configured microtremor array measurements (MAMs) for the geological investigation of underground space, Underground Space, https://doi.org/10.1016/j.undsp.2020.01.004

Table 3
Summary of actual and estimated bedrock depth in Bukit Timah Granite formation.

Sl. No	Test site	Borehole #	Actual bedrock depth (m)	Estimated bedrock depth (m)	Difference between actual and estimated bedrock depth (m)
1.	Woodlands near SLE (Ave 12 exit)	6604	34.3	33.0	+1.3
2.		6605	39.9	35.0	+4.9
3.	Ang Mo Kio Park	50126	25.8	26.5	−0.7
4.		50118	25.5	26.0	−0.5
5.	Ang Mo Kio St 24	5056	31.0	30.5	+0.5
6.		50133	28.5	31.5	−3.0
7.	Ang Mo Kio 3&6	50136	13.9	22.0	−8.1
8.	Woodlands Ave 1	11456	45.5	47.5	−2.0
9.		11468	41.2	38.0	+3.2
10.	Woodlands Dr 19	ST0008	24.2	27.0	−2.8
11.	Woodlands St 81	ST2012	31.0	31.1	−0.1
12.	Woodlands St 12	ST2014	18.5	25.0	−6.5
13.	Ang Mo Kio	RC/50130	28.2	33.0	−4.8
14.	Ang Mo Kio Park*	RC/5019	25.0	32.0	−7.0
15.	Republic Polytechnic	ST/4161	27.0	32.0	−5.0

Notes: *Presence of Kallang layer; SLE means Seletar Expressway; (−) indicates underestimation; (+) indicates overestimation.

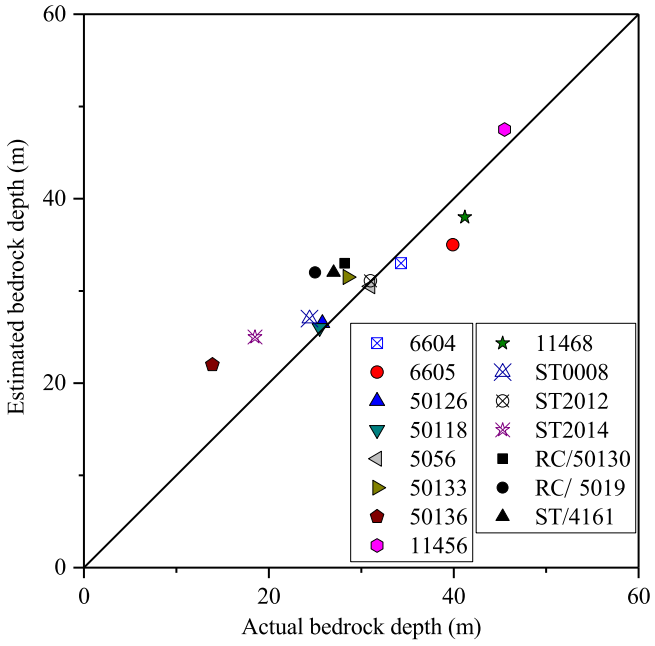

Fig. 7. Actual bedrock and estimated bedrock depth using V_s-based approach (500 m/s) at Bukit Timah Granite formation.

is subsequently conducted to derive the confidence interval of the variance. With these, the confidence interval for the prediction error can be determined and is superimposed on the scatter plot in Fig. 9. The blue and red dashed lines in Fig. 9 represent the 80% and 90% confidence intervals, respectively. Based on the scatter plot, it is observed that the MAM approach tends to give a better prediction if the bedrock depth is from 25 to 35 m. The confidence intervals of 80% and 90% indicate that the MAM approach is expected to predict a soil/rock interface within a +4.3 m/−6.4 m difference for the 80% case, and a +5.2 m/−6.7 m difference for the 90% case. Based on the

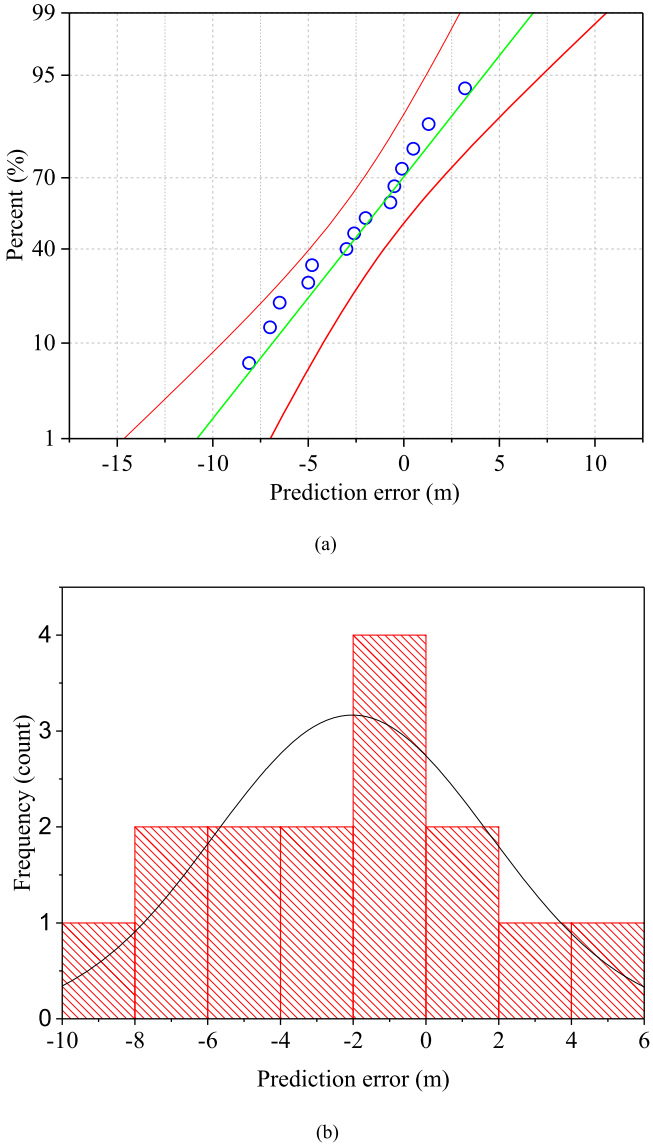

Fig. 8. Prediction error of MAM for Bukit Timah Granite formation: (a) cumulative probability density plot of the prediction error, and (b) histogram of probability density plot of prediction error.

Please cite this article as: T. Ku, S. Palanidoss, Y. Zhang et al., Practical configured microtremor array measurements (MAMs) for the geological investigation of underground space, Underground Space, https://doi.org/10.1016/j.undsp.2020.01.004

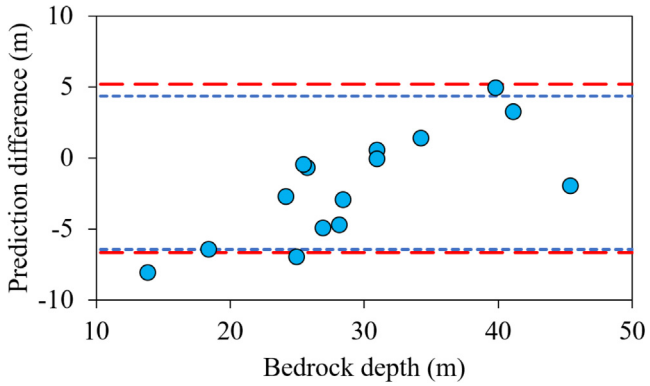

Fig. 9. Scatter of prediction error by MAM approach for Bukit Timah Granite formation. Blue and red dashed lines represent the 80% and 90% confidence intervals, respectively.

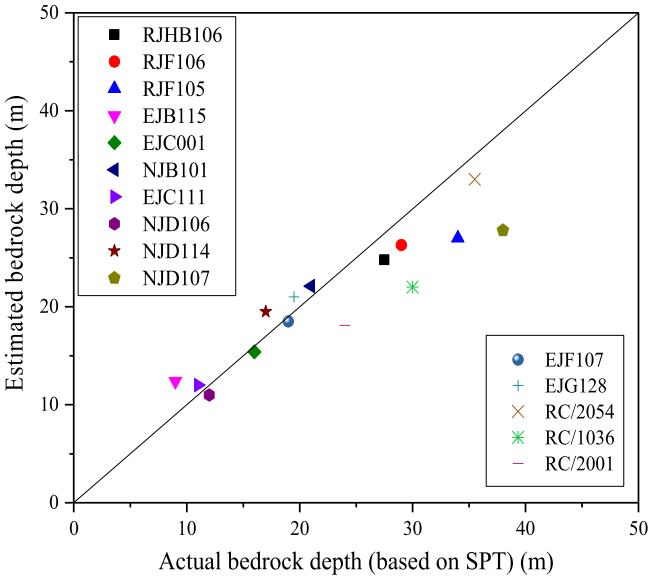

Fig. 10. Actual and predicted bedrock depth by MAM approach for Jurong formation.

results, it is expected that the proposed MAM approach can reasonably predict a soil/rock interface.

5.2 Jurong sedimentary formation

In this part of the study, 15 MAM tests were conducted in the western areas of Singapore within the Jurong formation. As explained in Section 4, a V_s of 500 m/s was used for estimating the soil/rock interface. Figure 10 compares the actual soil/rock interface and the estimation from the preselected V_s-based approach. Table 4 summarizes the actual soil/rock interface and the deviation from the estimated bedrock depth using the preselected V_s-based approach.

To assess the performance of the MAM approach, a statistical analysis is conducted (again). For the one-to-one plot shown in Fig. 10, hypothesis testing is performed if the prediction is equal to the actual measurement, with a significance level of 0.05. The hypothesis testing is passed, so it is reasonable to claim that the proposed MAM approach can predict the soil/rock interface. To establish a sense of accuracy associated with the confidence probability, the confidence interval is calculated. Based on the normality test, it is also confirmed that the prediction residuals follow a normal distribution, with a mean of −1.9 m and a standard deviation of 4.2 m. Figure 11(a) presents the cumulative probability density plot with the 95% confidence interval; Fig. 11(b) shows the histogram plot of the frequency of the prediction error and the fitted normal distribution probability plot.

A one-sample t test is conducted to determine the confidence of the mean, assuming the variance is unknown. The confidence interval for the prediction error is superimposed on the scatter plot shown in Fig. 12. The blue and red dashed lines in Fig. 12 represent the 80% and 90% confidence intervals, respectively. Interestingly, the scatter plot shows that the MAM approach tends to give different prediction accuracies in terms of the soil/rock interface (e.g., less residuals between 10 m and 20 m deep). The confidence intervals of 80% and 90% indicate that the MAM approach is expected to predict the bedrock within a +9 m/−3 m difference for the 80% interval, and a +9.9 m/−3.3 m difference for the 90% interval.

6 Discussion

In this section, we address two special scenarios that we encountered in the course of study. One is the effect of the presence of soft deposits. The other is the presence of overwhelming ambient noise. In addition to investigating the specific limitations of these two circumstances, we also discuss other possible generic limitations.

6.1 Effect of presence of soft deposit

In the course of detailed analysis, we observed that most dispersion curves follow a narrow band in the phase velocity and frequency domain, as shown in the blue area in Fig. 13. However, we also encountered a few special cases that fall in the pink and yellow zones. In this section, we discuss the specific scenario of the yellow zone, which is believed to be associated with the presence of a soft soil deposit (e.g., a Kallang formation).

As most of the dispersion curves measured in the study are within the blue zone, we denote them as the "normal dispersion" group. These cases typically involve residual soil, completely weathered soil, and rock masses with different weathering grades. We encountered three cases (shown in the yellow zone) that are rather distinguished from the normal dispersion group. The yellow zone, in turn, corresponds to a lower dispersion group. All three sites were found to have the presence of a soft deposit. A soft deposit is expected to a have lower stiffness (i.e., lower V_s) than the residual soils of Bukit Timah Granite and Jurong formations. Therefore, it can result in a dispersion

Please cite this article as: T. Ku, S. Palanidoss, Y. Zhang et al., Practical configured microtremor array measurements (MAMs) for the geological investigation of underground space, Underground Space, https://doi.org/10.1016/j.undsp.2020.01.004

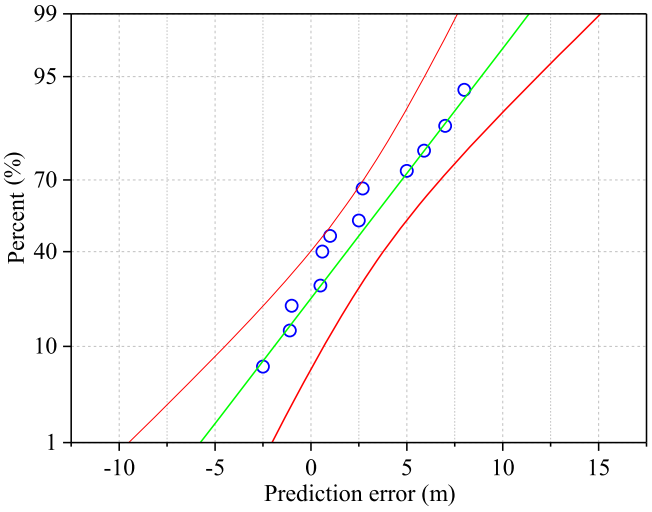

(a)

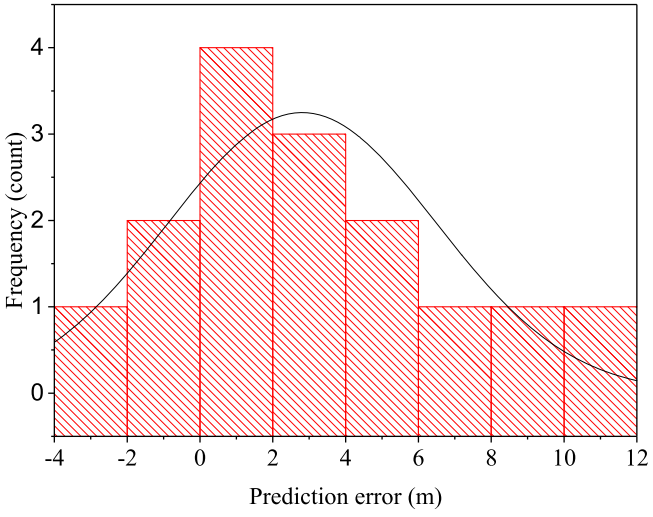

(b)

Fig. 11. Prediction error of MAM for Jurong formation: (a) cumulative probability density plot of the prediction error, and (b) histogram of probability density plot of prediction error.

curve in the lower dispersion group. In this zone, the pre-selected V_s for distinguishing the soil/rock interface is expected to be lower than 500 m/s, and should be carefully reviewed and calibrated when more testing results are available in future.

6.2 Effect of presence of overwhelming ambient noise

This section discusses another special scenario, i.e., the pink zone shown in Fig. 13. It denotes a higher dispersion group. In this zone, the testing sites share a common condition, i.e., that there was an intense ambient noise just next to the geophone array. For these cases, the ambient noise is not regularly balanced, but rather is overwhelmed by fully loaded container trailers and/or mass rapid transit

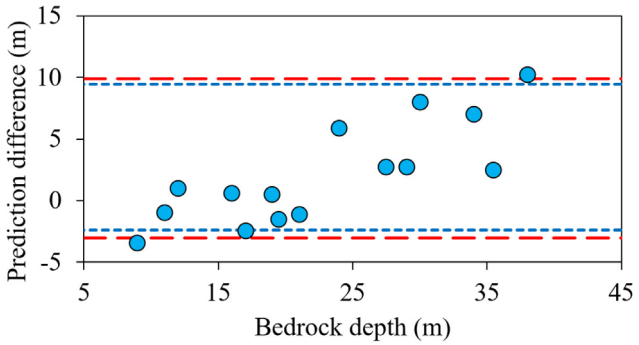

Fig. 12. Scatter of prediction error by MAM approach for Jurong formation (based on SPT rebound). Blue and red dashed lines represent the 80% and 90% confidence intervals, respectively.

trains. This influences the dispersion curve to exhibit the features of higher-mode surface waves. Hence, the dispersion curves for higher modes are analyzed. The same experimental dispersion curve can be reanalyzed by assuming it as a 2nd higher mode.

For instance, Fig. 14(a) shows the V_s profiles derived from the fundamental mode and 2nd higher mode for the test location at the Benoi-Pioneer Road Junction (RC/1036). There is a significant difference in the V_s profiles with depth. The estimated soil/rock interface using the 2nd higher mode inversion is 30.5 m, which is very close to the actual depth (30 m). Similarly, the 2nd higher mode inversion was performed for the test location of Jalan Buroh (RC/2001). Figure 14(b) compares the V_s profiles of the fundamental mode and 2nd higher mode at the borehole location RC/2001. The residual value of the actual-estimated soil/rock interface is 0.5 m. This clearly shows the effect of the overwhelming ambient noise. In such cases, the higher mode of the dispersion curves may be apparent, rather than the common fundamental mode. Therefore, it is advisable to perform a higher mode inversion.

6.3 Other limitations

In addition to the previous two specific scenarios, we discuss other possible and/or generic limitations below.

- MAM requires a 2D geophone array with a length of up to double the depth of interest. This is often not desirable for implementation, if such a site condition is not allowed or is constrained.
- The topography should be as flat as possible. However, uneven or slop ground surfaces may be encountered in real projects. If its elevation difference is significant, the MAM approach may not be suitable.
- A fundamental assumption of lateral homogeneity underlies the dispersion inversion. In the event of drastic variations in the subsurface layers within the array coverage, this fundamental assumption no longer holds. Figure 15 shows a boxplot of the MAM prediction difference with the actual soil/rock interface variation, based on all the testing sites. It clearly demonstrates

Please cite this article as: T. Ku, S. Palanidoss, Y. Zhang et al., Practical configured microtremor array measurements (MAMs) for the geological investigation of underground space, Underground Space, https://doi.org/10.1016/j.undsp.2020.01.004

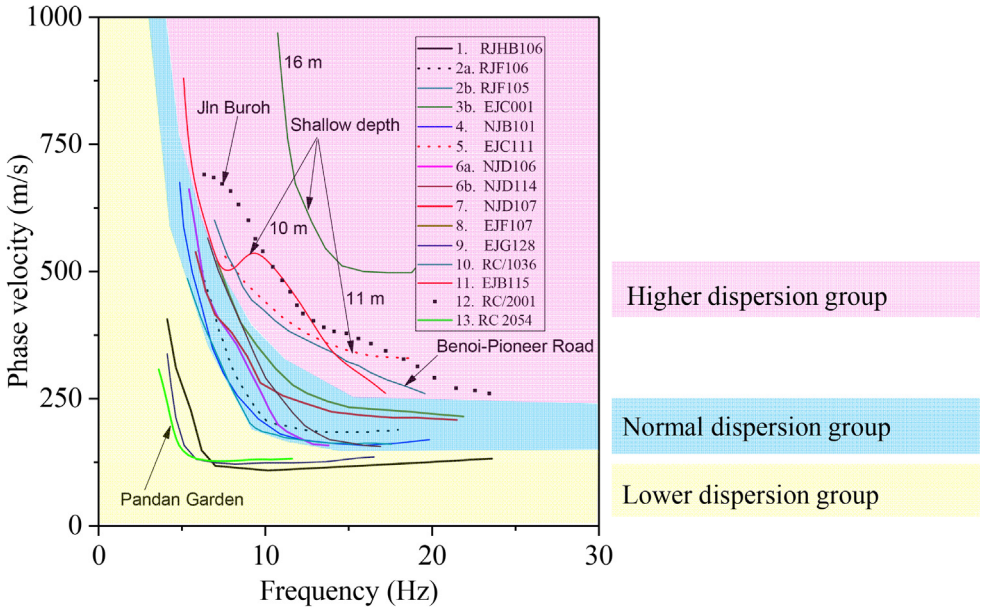

Fig. 13. Dispersion curves measured in Jurong formation with different groups.

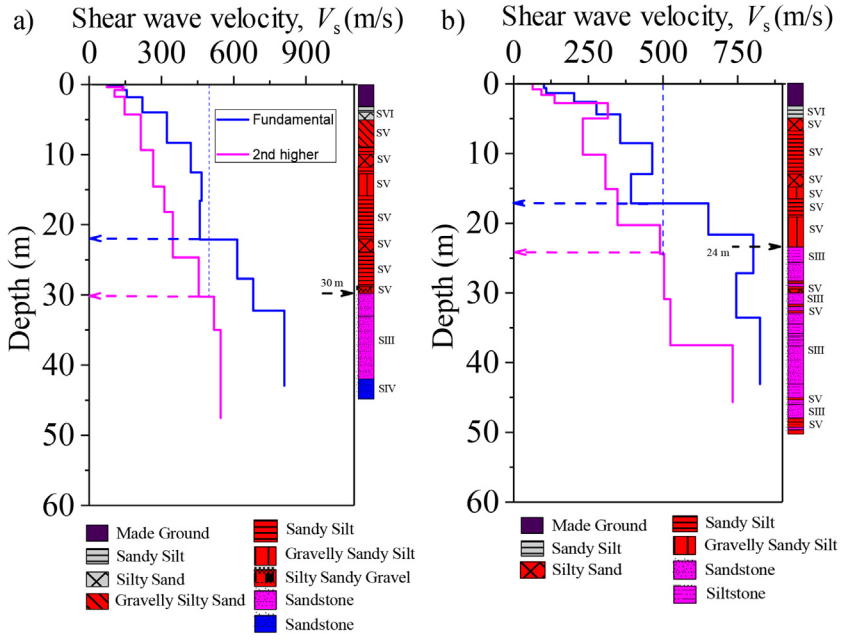

Fig. 14. Demonstration of higher mode inversion for higher dispersion group cases, (a) RC/1036, and (b) RC/2001.

the importance of holding this fundamental assumption. As such, MAM may not be desirable if the bedrock top varies dramatically on site.

- Finally, a dispersion inversion is a classic nonlinear and non-unique inverse problem. To partially solve the initial model-building problem, we constrain the initial model with the reference of the dispersion curve, by converting it to depth based on the wavelengths and phase velocity.

7 Conclusion

In this study, we investigated the feasibility of the practical application of non-invasive seismic geophysical testing for soil/rock interface evaluation at two major geological formations in Singapore, focusing on MAM (popularly known as the passive MASW test). Based on the testing results summarized in previous sections, the following conclusions and recommendations are made.

Please cite this article as: T. Ku, S. Palanidoss, Y. Zhang et al., Practical configured microtremor array measurements (MAMs) for the geological investigation of underground space, Underground Space, https://doi.org/10.1016/j.undsp.2020.01.004

Table 4
Summary of actual and estimated bedrock depth in Jurong formation.

Sl. No	Test site	Borehole #	Actual bedrock depth (m)	Estimated bedrock depth (m)	Difference between actual and estimated bedrock depth (m)
1	Jurong Central Park	RJHB106	27.5	24.8	+2.7
2	Jalan Boonlay	RJF106	29.0	26.3	+2.7
3		RJF105	34.0	27.0	+7.0
4	PIE Road	EJB115	9.0	12.4	−3.4
5		EJC001	16.0	15.4	+0.6
6	Jurong West Street 82	NJB101	21.0	22.1	−1.1
7	PIE Road	EJC111	11.0	12.0	−1.0
8	NTU1	NJD106	12.0	11.0	+1.0
9		NJD114	17.0	19.5	−2.5
10	NTU2	NJD107	38.0	27.8	+10.2
11	Jurong Town Hall Road	EJF107	19.0	18.5	+0.5
12	West Coast Road	EJG128	19.5	21.0	−1.5
13	Pandan Garden	RC/2054	35.5	33.0	+2.5
14	Benoi-Pioneer Rd Junction^	RC/1036	30.0	22.0	+8.0
15	Jalan Buroh^	RC/2001	24.0	18.1	+5.9

Notes: ^ Presence of heavy vehicle movement; PIE means Pan-Island Expressway; NTU means Nanyang Technological University; Assumed the dispersion curve belongs to fundamental mode; (−) indicates underestimation; (+) indicates overestimation.

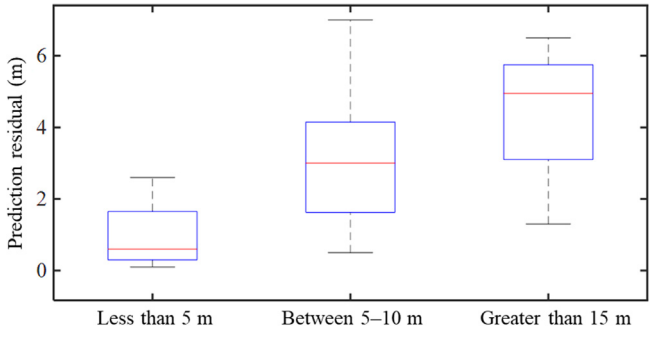

Fig. 15. Boxplot of prediction difference with the actual bedrock variation. Red lines indicate median values, whereas the blue box boundary represents the 1st and 3rd quartile.

- In urban environments, an L-shaped array/angular array of 90–135° is suggested for easy implementation of the MAM test.
- A shear wave velocity (V_s) of 500 m/s is recommended as a guide value for estimating the soil/rock interfaces for both the Bukit Timah Granite and Jurong formations.
- The presence of soft deposits considerably shifts the dispersion curve to the lower phase velocity (<400 m/s), reducing the V_s profile. In such cases, the proposed approach may not work with the guide value. Further investigation is needed.
- The effect of overwhelming ambient noise, such as from heavily loaded vehicles or trains, may significantly affect the results. In this case, a higher mode dispersion curve may be dominant, rather than a fundamental mode. Expertise is required to investigate this issue in depth to identify the order of the higher mode.
- The comprehensive MAM raw testing data and processed results can be used to contribute to a digital geology database for future applications.

Declaration of Competing Interest

The authors declare that they have no known competing financial interests or personal relationships that could have appeared to influence the work reported in this paper.

Acknowledgement

We acknowledge Land Transport Authority Singapore to fund this research project, using the land transportation innovation fund project: non-invasive geophysical study for bedrock evaluation (Award Number: R-302-000-164-490).

References

Aki, K. (1957). Space and time spectra of stationary stochastic waves, with special reference to microtremors. *Bulletin of the Earthquake Research Institute., 35*, 415–456.

Anderson, N. L., Croxton, N., Hoover, R., & Sirles, P. (2008). Geophysical methods commonly employed for geotechnical site characterization. Transportation Research Circular, (E-C130).

Brown, L., Diehl, J. G., & Nigbor, R. L. (2000). A simplified procedure to measure average shear-wave velocity to a depth of 30 meters (VS30). In Proceedings of 12th world conference on earthquake engineering. Auckland, New Zealand.

BSI (1999). *BS 5930: Code of practice for site investigations*. UK: BSI London.

Dal Moro, G., Pipan, M., & Gabrielli, P. (2007). Rayleigh wave dispersion curve inversion via genetic algorithms and marginal posterior probability density estimation. *Journal of Applied Geophysics, 61*(1), 39–55.

Galiana-Merino, J. J., Rosa-Cintas, S., Rosa-Herranz, J., Garrido, J., Peláez, J., Martino, S., & Delgado, J. (2016). Array measurements adapted to the number of available sensors: Theoretical and practical approach for ESAC method. *Journal of Applied Geophysics, 128*, 68–78.

Hayashi, K. (2008). Development of surface-wave methods and its application to site investigations. (Doctoral Dissertation), Kyoto University.

Ling, S. (1993). An extended use of the spatial autocorrelation method for the estimation of geological structure using microtremors. In Proceedings of the 89th SEGJ conference, 1993 (pp. 44–48).

Moon, S. W., Hayashi, K., & Ku, T. (2017a). Estimating spatial variations in bedrock depth and weathering degree in decomposed granite from surface waves. *Journal of Geotechnical and Geoenvironmental Engineering, 143*(7), 04017020.

Moon, S. W., & Ku, T. (2017b). Estimation of bedrock locations and weathering degree using shear wave velocity-based approach. In Proceedings of the 19th International Conference on Soil Mechanics and Geotechnical Engineering (ICSMG), Seoul, South Korea (pp. 627–630).

Moon, S. W., Subramaniam, P., Zhang, Y., Vinoth, G., & Ku, T. (2019). Bedrock depth evaluation using microtremor measurement empirical guidelines at weathered granite formation in Singapore. *Journal of Applied Geophysics, 171*. 103866.

Nazarian, S., & Stokoe, K. H. (1984). Nondestructive testing of pavements using surface waves. *Transportation Research Record, 993*, 67–79.

Okada, H., & Suto, K. (2003). The microtremor survey method. *Society of Exploration Geophysicists*.

Park, C. B., Miller, R. D., & Xia, J. (1999). Multichannel analysis of surface waves. *Geophysics, 64*(3), 800–808.

Subramaniam, P., Zhang, Y., & Ku, T. (2019). Underground survey to locate weathered bedrock depth using noninvasive microtremor measurements in Jurong sedimentary formation, Singapore. *Tunnelling and Underground Space Technology, 86*, 10–21.

Tokimatsu, K., Shinzawa, K., & Kuwayama, S. (1992). Use of short-period microtremors for V S profiling. *Journal of Geotechnical Engineering, 118*(10), 1544–1558.

Woon, L. K., & Yingxin, Z. (2009). *Geology of Singapore*. Defence Science and Technology Agency.

Xiang, Y., Liu, H., Zhang, W., Chu, J., Zhou, D., & Xiao, Y. (2018). Application of transparent soil model test and DEM simulation in study of tunnel failure mechanism. *Tunnelling and Underground Space Technology, 74*, 178–184.

Zhang, W., Zhang, R., Wu, C., Goh, A. T. C., Lacasse, S., Liu, Z., & Liu, H. (2019). State-of-the-art review of soft computing applications in underground excavations. *Geoscience Frontiers*. https://doi.org/10.1016/j.gsf.2019.12.003.

Zhang, Y., Li, Y. E., & Ku, T. (2019a). Geotechnical site investigation for tunneling and underground works by advanced passive surface wave survey. *Tunnelling and Underground Space Technology, 90*, 319–329.

Zhang, Y., Li, Y. E., Zhang, H., & Ku, T. (2019b). Near-surface site investigation by seismic interferometry using urban traffic noise in Singapore. *Geophysics, 84*(2), B169–B180.

Zhao, J., Liu, Q., Lee, K., Choa, V., & Teh, C. (1999). Underground cavern development in the Jurong sedimentary rock formation. *Tunnelling and Underground Space Technology, 14*(4), 449–459.

Please cite this article as: T. Ku, S. Palanidoss, Y. Zhang et al., Practical configured microtremor array measurements (MAMs) for the geological investigation of underground space, Underground Space, https://doi.org/10.1016/j.undsp.2020.01.004